

Synthesis of diatomite Silica Doped Iron Nanoparticle Innovative Material Composite and their Enhanced Photocatalytic Activity Driven by UV Light

REZIG Walid

Laboratoire des Sciences, Technologie et Génie des Procédés LSTGP ; Faculté de Chimie ; Département de Génie Chimique ; Université des Sciences et de la Technologie d'Oran Mohamed Boudiaf USTO-MB ; BP 1505 El Mnaoueur Bir El Djir 31000 Oran Algeria

Oran, Algeria

walidrzg@gmail.com / walid.rezig@univ-usto.dz

HADJEL Mohammed

Laboratoire des Sciences, Technologie et Génie des Procédés LSTGP ; Faculté de Chimie ; Département de Chimie Organique Industrielle ; Université des Sciences et de la Technologie d'Oran Mohamed Boudiaf USTO-MB ; BP 1505 El Mnaoueur Bir El Djir 31000 Oran Algeria

Oran, Algeria

hadjel100@yahoo.fr

Abstract—Diatomite silica doped iron nanoparticle thermally calcination at 600 °C “ DMF3X6 ” composite as catalyst for heterogeneous photocatalysis of vat green 03 indanthren and characterized in this study. The Diatomite silica doped iron nanoparticle thermally calcination at 600 °C called “ DMF3X6 ” was made through surface modification treatment including NaOH deposition on raw diatomite with thermally calcination. In NaOH treatment, surface of Diatomite silica doped iron nanoparticle thermally calcination at 600 °C “ DMF3X6 ” was partially dissolved in NaOH with thermally calcination at 600 °C by means of x-ray fluorescence (XRF), x-ray diffraction (XRD), attenuated reflection-Fourier transform infrared (ATR-FTIR), scanning electron microscopy (SEM), energy dispersive x-ray (EDX), thermogravimetric analysis (TGA), differential scanning calorimetry (DSC) and UV-visible diffuse reflectance spectroscopy (DRS). The surface area of Diatomite silica doped iron nanoparticle thermally calcination at 600 °C “ DMF3X6 ” is 218.2 m²/g. The band gap of DMF3X6 was $E_g = 1.15$ eV by UV-visible DRS technique. The surface modification also increased the point of zero charge (pH_{PZC}) values to 6 for Diatomite silica doped iron nanoparticle thermally calcination at 600 °C “ DMF3X6 ”. The vat green 03 indanthren textile dye degradation has pH dependency, the better result is at pH =10 with colour remove about 92 %. The photodecolourisation rate follows pseudo-first order kinetic with respect to the dye concentration.

Keywords—Diatomite, silica, iron, composite, heterogeneous photocatalysis, band gap, dye degradation, UV irradiation, photodecolourisation.

I. INTRODUCTION

Diatomite is a natural amorphous silica with chemical formula ($SiO_2 \cdot nH_2O$). Diatomite is a siliceous rocks very light and

porous formed mainly by accumulation of frustules [1,2]. Treated thermally diatomite is used for the removal of textile dyes [3,4]. The natural ferric oxide contains many phases and characterized crystallinity as: ferrihydrite, maghemite, lepidocrocite, hematite and goethite [5]. Diatomite modified by ferrihydrite is an adsorbent with sodium hydroxide NaOH and ferrous chloride tetrahydrate $FeCl_2 \cdot 4H_2O$ deposition into raw diatomite RD [6]. Textile dyes are an environmental contaminants with their potential toxicity cause a pollution of water sources [7,8]. Vat dyes from textile industry cause a carcinogenic health effects [9]. Photocatalysis is one of advanced oxidation process to remove an organic contaminants [10]. The advantage of amorphous silica is used to prepare a supported catalysts [11,12]. Hematite is a semiconductor with band gap range between 1.9 and 2.2 eV [13]. Silica doped by hematite is used as a photocatalyst by sol-gel method [14]. Silica from diatomite doped iron nanocomposite as photocatalyst to produce the radical hydroxiles and to remove the organic pollutants [15,16].

So this study, vat green 03 indanthren removal by photodegradation method using diatomite SiO_2 doped iron nanoparticle by thermally calcination (Diatomite SiO_2 -Fe) as photocatalyst to degrade vat green 03 indanthren dye textile under UV irradiation.

II. MATERIALS AND METHODS

A. Natural diatomite

Natural diatomite was obtained from Sig deposit located in the westward of Algeria. The chemical composition of raw diatomite RD studied was determined by x-ray fluorescence X (XRF) (Philips PW 1404) and by electronic Micro sounder

based on chemical analysis by x-ray fluorescence x (XRF) (Philips PW 1404).Raw diatomite RD in powder is composed of 68.017 % SiO_2 , 19.25 % CaO , 7.575 % Al_2O_3 ; 2.022 % Fe_2O_3 ;1.241 % MgO ; 1.491 % K_2O ; 0.2 % Na_2O ; 0.14 % TiO_2 and 0.038 % MnO and 0.5 % others [17] as shown in Fig.1.



Fig.1. The raw diatomite RD in powder

B. Preparation of diatomite silica doped iron oxide nanoparticle

RD sample (45 g) was immersed in 300 ml 6M NaOH [18] solution at 90 °C for 2 h to partially dissolve Si [15] .The mixture was immediately added to 300 ml of $\text{FeCl}_2 \cdot 4\text{H}_2\text{O}$ solution with 3 M concentration and stirred (see Fig.2) and oxidized in air at room temperature (25 °C) for 24 h (see Fig. 3). The mixture was centrifuged for 30 min with the speed of 12000 rotations/min for assured the separation.The solid obtained through centrifugation was washed with distilled water and oxidized in air at room temperature overnight.The mixture was centrifuged for 30 min with the speed of 15000 rpm (rotations per minute) for assured the separation to remove excess NaOH. The solid obtained through centrifugation was washed with distilled water and oxidized in air to continue the oxidation $\text{Fe}(\text{OH})_2$ and remove the excess of NaOH for 24h. The mixture was dried at 105 °C for 24h [17] . During the experimental procedure, diatomite sample was created and tested: diatomite thermally modified at 600 °C for 24 in oven (see Fig.4) . The products of this procedure were named DMF3X6 as shown in Fig.5.



Fig.2. Diatomite silica doped iron nanoparticle with thermally calcination at 600 °C (DMF3X6) during stirring and heating

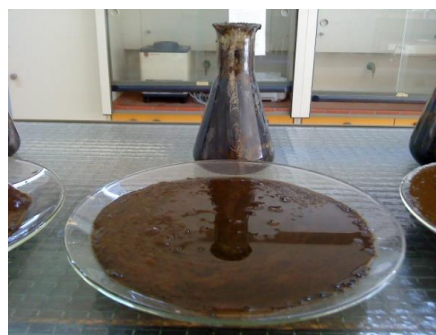


Fig.3. Diatomite silica doped iron nanoparticle washed by distillate water and oxidized in air at room temperature at 24 h



Fig.4. Diatomite silica doped iron nanoparticle with thermally calcination at 600 °C (DMF3X6) in oven



Fig.5. Diatomite silica doped iron nanoparticle with thermal calcination at 600 °C (DMF3X6) in powder

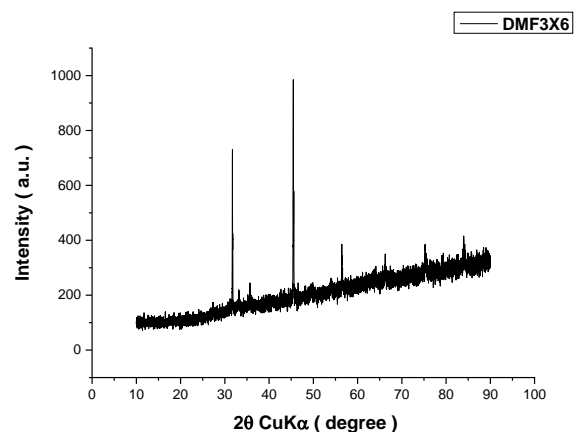


Fig.6. X-ray diffraction patterns of Diatomite silica doped iron nanoparticle thermally calcination at 600 °C “DMF3X6”

III. RESULTS AND DISCUSSION

A. X-ray fluorescence (XRF)

The mineralogical composition of diatomite silica doped iron nanoparticle with thermal calcination at 600 °C (DMF3X6) studied was determined by quantified x-ray fluorescence in the form of oxides and is reported in Table I.

TABLE I. Mineralogical analysis in percentages by % weight of Diatomite silica doped iron nanoparticle with thermal calcination at 600 °C (DMF3X6)

Composants	SiO ₂	Fe ₂ O ₃	Al ₂ O ₃	CaO	MgO	K ₂ O	TiO ₂	P ₂ O ₅	SO ₃	LOI
(%) weight	37.27	20.14	3.42	1.56	1.30	1.25	0.25	0.21	0.14	34.46

TABLE I shows XRF analysis result. For DMF3X6 shows the dominance two oxides are : 37.27 % SiO₂ and 20.14 % Fe₂O₃ and others oxides with low weight percentages and loss by ignition (LOI) as 34.46 %.

B. X-rays diffraction (XRD) studies

The mineralogy of diatomite biosilica doped iron nanoparticle thermal calcination at 600 °C “DMF3X6” was characterized by powder x-ray diffraction (XRD) analysis using a model Bruker D8 ADVANCE x-ray diffractometer (Germany) Cu Kα radiation (λ = 0.1540598 nm, 50 kV, 100 mA). The powder sample was coated on a plate out of glass of methanol and was dried with the room temperature, then swept 1° with 80° (2θ) with the size of stage of 0.020° as shown in Fig.6.

The peaks at 14.1°-35.7°-43°-45.5°-49.5°-51.4°-56.5° with d= 6.28-2.51-2.1-1.99-1.84-1.77-1.62 correspond kaolinite (Al₂Si₂O₅(OH)₄) (ASTM 14-164). The peak at 24.1° with d=3.69 corresponds quartz (SiO₂) [19,20]. The peaks at 45.5°-51.4°-56.5°-66.2° with d = 1.99-1.77-1.62-1.40 correspond quartz (SiO₂) (ASTM 5-490) [21]. The peaks at 31.6°-45.5°-56.5°-66.2° with d= 2.82-1.99-1.62-1.40 corresponds calcite (CaCO₃) (ASTM 5-490) [20]. The peak at 54.1° with d= 1.69 corresponds rutile (TiO₂) (ASTM 5-551) [21]. The peaks at 35.7°-45.5° with d=2.51-1.99 correspond illite, ((K,H₃O),(Al,Mg,Fe)₂O₁₀((OH)₂,H₂O)) (ASTM 9-343). The peaks at 35.7°-54.1° with d=2.51-1.69 correspond hematite (α-Fe₂O₃) (ASTM 8-98). The peaks at 35.7°-43°-56.5° with d = 2.51-2.12-1.62 correspond magnetite (Fe₃O₄) (ASTM 8-98) [37,38]. The peak at 43° with d=2.1 corresponds maghemite (γ-Fe₂O₃) [21]. The peak at 43° with d=2.1 corresponds lepidocrocite (γ-FeOOH) (ASTM 8-98) [21]. The peaks at 49.5°-54.1° with d= 1.84-1.69 correspond anatase (TiO₂) (ASTM 4-447). The peak of anatase TiO₂ appear at 24.1°-49.5° with d=3.69-1.84 which are consistent with the value in the standard card (JCPDS N° 21-1272). There two reflections at 35.7°-66.2° with d= 2.51-1.40 found in the XRD pattern of diatomite silica doped iron nanoparticle thermal calcination at 600 °C “DMF3X6” indicate that the Fe₂O₃ deposited into their diatomite is the least crystalline ferrihydrite (2-line ferrihydrite) with higher surface area and site density than other iron (III) oxides [23,24]. The peak at 24.1°-49.5° with d= 3.69-1.84 as a peak of anatase TiO₂ character in accordance with anatase standard (JCPDS 12-1276). The peak at 35.7°-54.1° with d=2.51-1.77 correspond the Fe₂O₃ [25]. In the XRD pattern of Fe₃O₄, the diffraction angles 35.7°-43°-54.1°-56.5° with d= 2.51-2.1-1.77-1.62 corresponded to the crystal surface of Fe₃O₄ [26,27]. In XRD patterns of the loaded catalyst, although the intensity

of lines decreased due to Fe-O loading was observed at 43° with $d=2.1$ nm shows formation of Fe-O [28]. The peaks at 33.2° - 35.7° - 43° - 54.1° with $d=2.7$ - 2.51 - 2.1 - 1.69 nm correspond to goethite (α -FeOOH) (JCPDS card 29-0713). The spectra of the constituents we have formed present a peak at 24.1° - 33.2° - 35.7° - 43° - 49.5° - 54.1° , which can be attributed to hematite (α -Fe₂O₃) [29].

C. Attenuated Total Reflectance Fourier Transform Infrared (ATR-FTIR) Spectroscopy

The ATR-FTIR spectra of diatomite silica doped iron nanoparticle thermally calcination at 600°C "DMF3X6" is realized with help of spectrophotometer using a model Bruker Alpha H GmbH D8 Attenuated Total Reflectance - Fourier Transform Infrared Spectrometer (ATR-FTIR) between 4000 cm^{-1} and 400 cm^{-1} with the resolution of 4 cm^{-1} ; 28 scans were performed. The sample is conditioned with the dispersion form in the powder of diatomite silica doped iron nanoparticle thermally calcination at 600°C "DMF3X6". The result is shown in Fig.7.

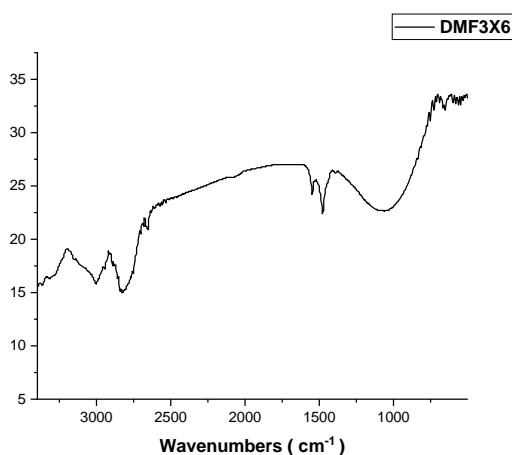


Fig.7. ATR-FTIR spectra of diatomite silica doped iron nanoparticle thermally calcination at 600°C "DMF3X6"

ATR-FTIR spectra (Fig.7) of diatomite silica doped iron nanoparticle thermally calcination at 600°C "DMF3X6" material display bands at 3398.47 and 1622.78 cm^{-1} that correspond to the O-H symmetric/antisymmetric stretchings, and H-O-H bending vibrations of adsorbed water molecules physically adsorbed on H-bonded silanol groups (Si-OH) present on diatomite surface [30]. The bands at 2349.59 and 1334.28 cm^{-1} are unambiguously assigned to C-O stretching mode ($\delta_{\text{C-O}}$) of calcium carbonate [30,31] that occurs in natural diatomite under aragonite and calcite phases. There is a new absorption band at 2071.60 cm^{-1} corresponds the vibration of silane group (Si-H) [32].

The broad band at 1065.68 and 806.23 cm^{-1} due to the presence of Si-O-Si species are well evident [33]. The bands at 1483.91 , 1431.31 cm^{-1} are unambiguously assigned to C-O stretching mode ($\nu_{\text{C-O}}$) of calcium carbonate [30,31]. That occurs in natural diatomite under aragonite and calcite phases. Furthermore ($\nu_{\text{C-O}}$), the relative high intensity of the bands situated at 1483.91 and 1431.31 cm^{-1} reveal a high content of calcium carbonate in sample [30,31]. Another contribution of water molecules within the sample is found at 1622.78 cm^{-1} which refers to the bending vibrations of O-H groups ($\delta_{\text{O-H}}$) of adsorbed water molecules [34]. The band at 3398.47 cm^{-1} refers to monomeric hydrogen bonds, which are assigned in diatomite silica doped iron nanoparticle thermally calcination at 600°C "DMF3X6" system to Fe-OH species present on surface. Indeed in the case of nano-hydroxylated atoms, the surface iron atoms tend to complete their coordination shell by reacting with water molecules in order to form surface Fe-OH species [35]. The latter observation is expected given the fact that oxo- and hydroxo-species demonstrate a high tendency to form hydrogen bonds extensively. Moreover, the spectral study gives more insight into the contribution of surface silanol groups in the formation of diatomite silica doped iron nanoparticle thermally calcination at 600°C "DMF3X6", which is suggested to occur by the establishment of strong covalent bonds between the iron species and these specific reactive sites [36,37] that spreads over frustule surface. The peak at 713.25 cm^{-1} and the band at 641.04 cm^{-1} related to Si-O-Fe [38] or Ti-O [39] and Fe-O-Fe bonds [38], respectively, disappeared due to the removal of metallic impurities from amorphous silica matrix. The band at 537.75 cm^{-1} is related to Fe-O stretching in maghemite [15,40] could be ascribed to Fe-O in Fe₂O₃, suggesting that Fe₂O₃ was connected with the diatomite sheets [58,59]. The band centred at 442.40 cm^{-1} is ascribed to the Si-O-Al antisymmetric bending [43,44].

D. Scanning Electron Microscopy with Energy Dispersive X-ray Spectroscopy (SEM-EDX)

The morphologies of the mineral phases constituting the samples were investigated by scanning electron microscopy equipped energy dispersive x-ray EDX using a model (JEOL JSM-6610La, Japan). The sample was first mounted flat, using carbon tape, and then coated with 30 nm of gold using a sputter coater, the working distance was set to 17 mm and then accelerating voltages of 20 kV were used.

Fig.8 shows an electronic micrograph of diatomite silica doped iron nanoparticle thermally calcination at 600°C "DMF3X6".

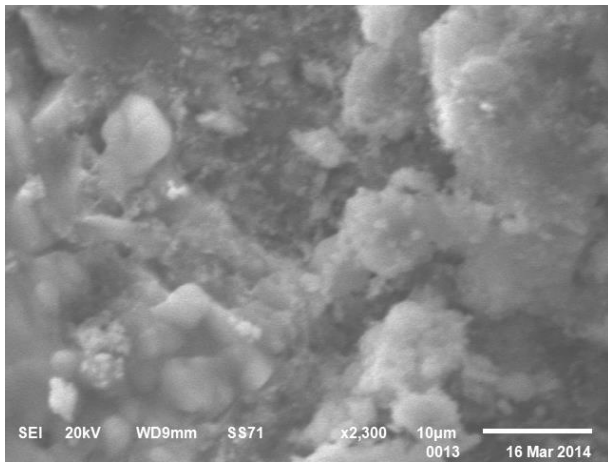
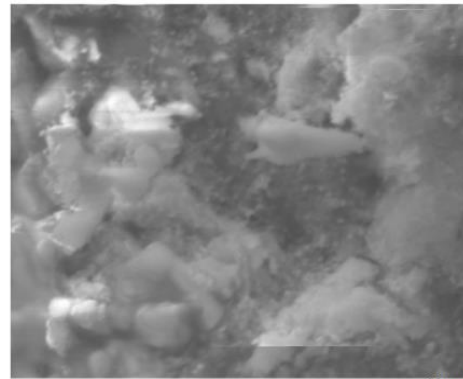


Fig.8. Scanning electron micrograph of diatomite silica doped iron nanoparticle thermally calcination at 600 °C “ DMF3X6 ” (magnification 2300 X)

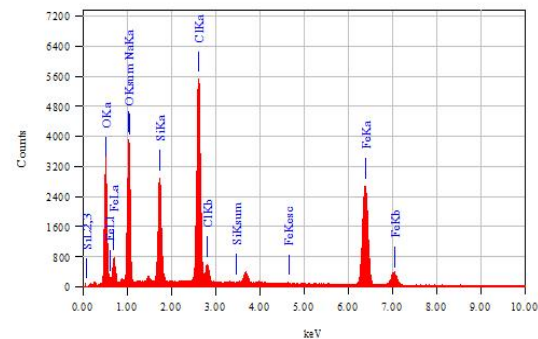
The SEM micrograph of diatomite silica doped iron nanoparticle thermally calcination at 600 °C “ DMF3X6 ” reveals that raw diatomite frustules are surface modified and the original geometry of the pores is destroyed by the FeCl₂.4H₂O and NaOH treatments (Fig.8.).The presence of the ferric oxyhydroxide phases detected on diatomite frustules [45,46] by SEM (Fig.8.).The SEM micrograph of diatomite silica doped iron nanoparticle thermally calcination at 600 °C “ DMF3X6 ” reveals that raw diatomite frustules are surface modified and the original geometry of the pores is destroyed by the NaOH treatment and the ferrihydrite deposition (Fig.8). Initially,colloidal-size ferrihydrite (2–5 nm) is deposited into the macropores (>50 nm) and larger mesopores (>7 nm) of diatomite.After being fully deposited into the pores of diatomite, extra ferrihydrite aggregates on the surface of diatomite particles (see Fig.8) [47].

Fig.9 represents a mass percentages estimated for elements (Fe, O, Na, Cl and Si) in diatomite silica doped iron nanoparticle by EDX are : Fe 50.53 % , O 22.41 % , Na 19.19 % , Cl 18.04 % in high mass percentages and and Si 8.12 % in low percentage mass (Fig.9).

View001



JEOL 1/1
Title : IMG1
Instrument : 6610(LA)
Volt : 20.00 kV
Mag. : x 2,300



Acquisition Parameter
Instrument : 6610(LA)
Acc. Voltage : 20.00 kV
Probe Current: 1.00000
PHA mode : T3
Real Time : 102.59
Live Time : 100.00
Dead Time : 2 %
Counting Rate: 2734 cps

ZAF Method Standardless Quantitative Analysis
Fitting Coefficient : 0.0590

Element	(keV)	Mass%	Sigma	Atom%	Compound	Mass%	Cation
Si K	1.739	8.12	0.06	8.01			
Cl K	2.621	18.04	0.08	14.09			
Na K	1.041	19.19	0.12	23.12			
O K	0.525	22.41	0.12	38.79			
Fe K	6.398	32.24	0.16	15.99			

JED-2300 AnalysisStation

JEOL

Fig.9. method standardless quantitative analysis estimated for elements (Fe, O, Na, Cl and Si) in DMF3X6 by EDX coupled with SEM are : Fe 50.53 % , O 22.41 % , Na 19.19 % , Cl 18.04 % and Si 8.12 %)

E. Thermal Analysis (TGA-DSC)

Thermogravimetric analysis (TGA) was carried out in a STD Q600 V.3 Build 101, TA instruments, U.S.A.) instrument at heating rate of 10°C/min, in the temperature range 0-1200 °C.The melting temperature and latest heat of diatomite silica doped iron nanoparticle thermally calcination at 600 °C “ DMF3X6 ” was determined by means of differential scanning calorimetry (DSC) (TA instrument DSC STD Q600 V.3 Build 101).In the temperature range 0-1200 °C at a heating cooling rate of 10 °C/min.

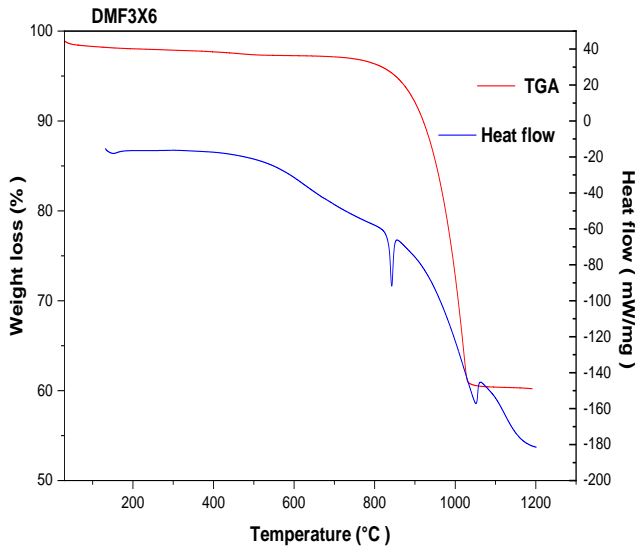


Fig.10. Thermal analysis (TGA-DSC) curves of diatomite silica doped iron nanoparticle thermally calcination at 600 °C “DMF3X6”

Fig.10 displays the TGA and DSC scans of diatomite silica doped iron nanoparticle thermally calcination at 600 °C “DMF3X6”. On heating, the DSC scan reveals the presence of two endothermic peaks at 795.28 °C ($\Delta H = 156.2$ J/g) and 1027.17 °C ($\Delta H = 465.4$ J/g) resulting both from the decomposition of the organic phase present on the surface of the silica of diatomite silica doped iron nanoparticle thermally calcination at 600 °C “DMF3X6” and optionally to the dehydroxylation of the silanol groups (Si-OH) during the raise of temperature [48]. The two phase transition or meeting temperature of diatomite silica doped iron nanoparticle thermally calcination at 600 °C “DMF3X6” is about 787.01 °C, with latent heat (156.2 J/g) and the second 942.69 °C, with latent heat (465.4 J/g) [49]. Above 300 °C, transformation ferrihydrite of DM3X6 to hematite ($\alpha\text{-Fe}_2\text{O}_3$) or recrystallization of hematite [50]. The final phase transition was achieved by completing the dehydroxylation step that overlaps with instantaneous crystallization of the end hematite product from a disordered or non-crystalline to crystalline ($\alpha\text{-Fe}_2\text{O}_3$) from [51-54].

F. Surface charge

The surface area of diatomite silica doped iron nanoparticle thermally calcination at 600 °C “DMF3X6”, was determined, according to Sears method [55], by weighing 0.5 g of DMF3X6, and acidifying with dilute hydrochloric acid to pH of 3-3.5. Sodium chloride (10g) was then added with stirring, and the mixture was made up to a total volume of 50 ml with distilled water. The solution was titrated with 0.1M sodium hydroxide NaCl and the pH measured throughout the titration process. The volume, V, required to increase the pH

from 4 to 9 was recorded. The surface area (S) was estimated from the equation (1) [18]:

$$S (\text{m}^2\text{g}^{-1}) = 32 V - 25 (1)$$

Where 32 and 25 are Sears empiric constants. The surface charge of diatomite silica doped iron nanoparticle thermally calcination at 600 °C “DMF3X6” was determined by a potentiometric titration method [56,57]. The same concentration of the DMF3X6, used in this manipulations are 1gL^{-1} were first placed in the shaker for 2h at room temperature. Titrations were then carried out by using 0.1 M hydrochloric acid and then 0.1 M sodium hydroxide, and the pH was measured throughout the titration process. The volume (ml) of acid or base needed to change the pH from 3 to 12 was recorded, duplicate samples were measured and the results were reported as an average. The surface area of diatomite silica doped iron nanoparticle thermally calcination at 600 °C “DMF3X6” used in this study was calculated by Sears method [55] as $218.2 \text{ m}^2/\text{g}$.

The surface charge density (C/m^2) is determined by the following [56,57]:

$$\sigma = (C_A - C_B + [\text{OH}^-] - [\text{H}^+]) F / A m \quad (2)$$

[56,57]

Where C_A and C_B are the concentration of acid and base needed to reach a point on the titration curve, in mol/L, $[\text{H}^+]$ and $[\text{OH}^-]$ are the concentrations of H^+ and OH^- converted from pH, in mol/L, F is the Faraday constant ($96490 \text{ C}/\text{mol}$), A is the specific surface area, in m^2/g , and m is the concentration of diatomite silica doped iron nanoparticle thermally calcination at 600 °C “DMF3X6”, in g/L. The surface charge of diatomite silica doped iron nanoparticle thermally calcination at 600 °C “DMF3X6” as function of solution pH is shown in Fig.11 and Fig.12. The titration curve illustrates that the surface charge decreases as the pH is increased. The intersection of two curves with x-axis gives the point of zero charge (pH_{PZC}) which was 6 for diatomite silica doped iron nanoparticle thermally calcination at 600 °C “DMF3X6”. In this study, at pH_{PZC} , the total charge from cations and anions at the sample surface is equal to zero. The surface charge is negative when the solution pH is above pH_{PZC} and becomes positive when pH below pH_{PZC} .

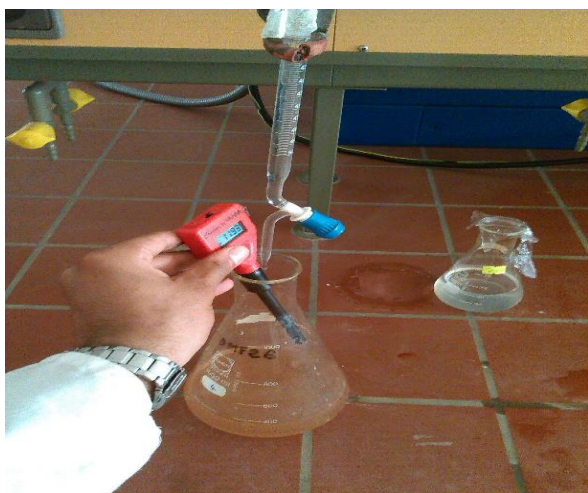


Fig.11. Potentiometric Titration Curve of diatomite silica doped iron nanoparticle thermally calcination at 600 °C “DMF3X6”

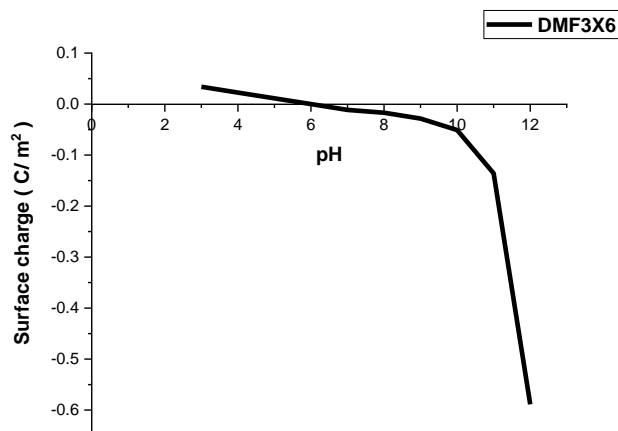


Fig.12. Curve of diatomite silica doped iron nanoparticle thermally calcination at 600 °C “DMF3X6” of Surface Charge in function of pH medium

The pH of the zero charge point pH_{PZC} of diatomite silica doped iron nanoparticle thermally calcination at 600 °C “DMF3X6” is equal to 6 as shown in Fig.12.

G. UV-visible -DRS analysis

UV-visible diffuse reflectance spectroscopy measurements were carried out using a Perkin Elmer Lambda 650 spectrophotometer equipped with an integrating sphere attachment. The analysis range was from 200 to 800 nm, and polytetrafluoroethylene (PTFE, Teflon) Was used as a reflectance standard. The Kubelka–Munk formalism and Tauc plots Were used to determine the band gap energy. The residual pollutant concentrations during degradation were monitored with Shimadzu UV mini-1240 spectrophotometer

in the range 200–800 nm, using 1 cm optical pathway cells. According to the Planck’s law and some further calculation, the relationship between the Absorption wavelength of the photoreactor and the band gap value can be determined By Eq. (3):

$$E_g = \frac{hc}{\lambda} = \frac{1239}{\lambda} \quad (3)$$

Where h is Planck’s constant ($4.13566733 \times 10^{-15}$ eV s : C is the speed of light ($2.99792458 \times 10^{17}$ nm s⁻¹) and λ is the UVA-light wavelength (320-380 nm). From the calculation, in order to absorb a UV-light wavelength, the band gap value of the photoreactor has to be below 3.87 eV and above 3.26 eV. Fig.13 shows UV-visible diffuse reflectance spectrum for DMF3X6 sample recorded in the wavelength range of 200-800 nm. The UV-visible absorption spectrum of diatomite silica doped nanoparticle thermally calcination at 600 °C “DMF3X6” compound was taken and subsequently its optical band gap was calculated using the Tauc approach Eq. (4) [58,59] :

$$\alpha h\nu \approx A (h\nu - E_g)^{n/2}$$

Where α , h , ν and A are the linear absorption coefficient, Planck’s constant, light frequency, band gap energy of the material and A constant involving properties of the bands, respectively. The exponent n depends on the type of transition between the semiconductor bands. The values of n for directly allowed, directly forbidden, indirectly allowed, or indirectly forbidden transition are $n = 1, 2, 3$ and 4 , respectively. By applying $n=4$, the indirect band gap (E_g) of the as-prepared photocatalyst is determined from the plot of $(\alpha h\nu)^{1/2}$ versus $h\nu$, as indicated in Fig.14. By Extrapolating the straight line to the x-axis in this plot, the E_g value of silica diatomite doped iron nanoparticle thermally calcination at 600 °C “DMF3X6” was found to be 1.15 eV. The estimates value indicates that DMF3X6 possessed narrower band gap and the optical transition for DMF3X6 was indirectly allowed [60].

dye of textile.

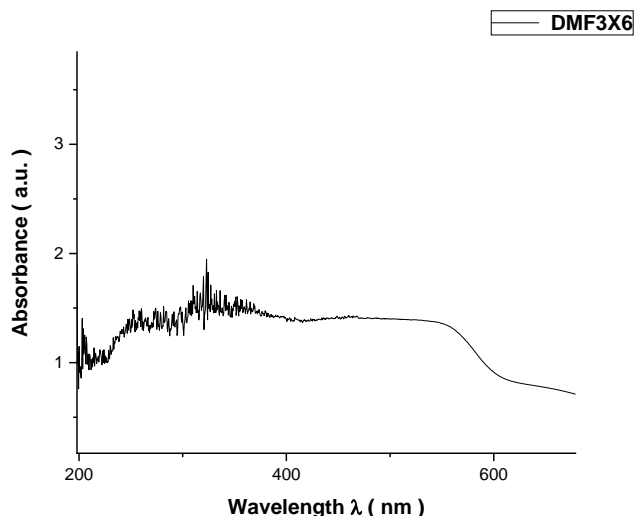


Fig.13. UV-visible diffuse reflectance spectrum for diatomite silica doped iron nanoparticle thermally calcination at 600 °C “ DMF3X6 ”

The Indanthrene Olive Green B (C.I.Vat Green 3 ; C.I.69500) VG3 dye of textile was obtained from an industrial textile treatment Essenia « SOTEXHAM » in Oran in the West of Algeria. The Fig.16 shows the solution of the indanthrene Olive Green B (C.I.Vat Green 03; C.I.69500) VG3 dye of textile.



Fig. 16.The solution of The Indanthrene olive Green B (C.I.Vat Green 3 ; C.I.69500) VG3 dye of textile

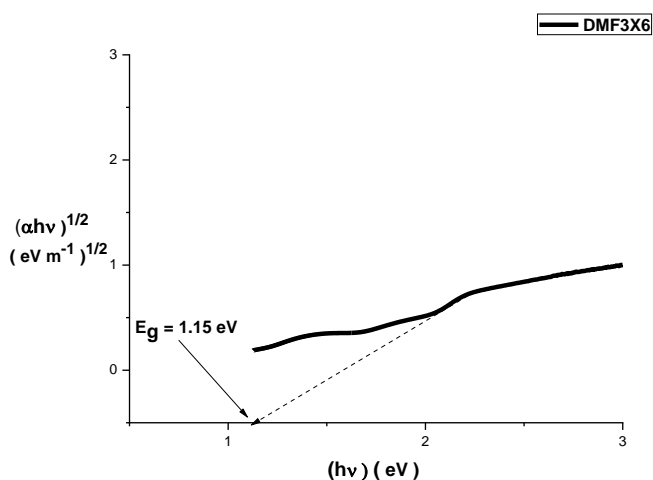


Fig.14. Plot of $(\alpha hv)^{1/2}$ against (hv) from the UV-vis diffuse reflectance for diatomite silica doped nanoparticle thermally calcination at 600 °C “ DMF3X6 ”.In the inset, the band gap value is described

H. Photocatalytic Activity

The Fig.15. represents the molecular structure of the Indanthrene Olive Green B « Vat Green 03 indanthren » dye of textile.

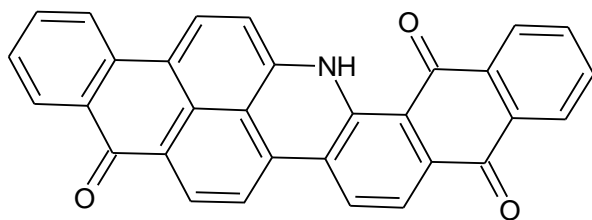


Fig. 15. Molecular structure of the Indanthrene Olive Green B « Vat Green 3 »

The objective for this work is to optimize the operating conditions of the photodegradation of titanium dioxide (Degussa P25) and diatomite silica doped iron nanoparticle thermally calcination at 600 °C “ DMF3X6 ” .For this we varied the pH of 4, 7 and 10 and the concentration of diatomite silica doped iron nanoparticle thermally calcination at 600 °C “ DMF3X6 ” is 0.5g /L and thus release industry and textile dye (Vat Green 03 indanthren), which is used as indicators of contamination at a concentration of 2.5 mg/L..The photocatalytic activity was determined based on the pH and the absorbance of samples after each 15 min.

Pollutants studied

the subject of this study contains the Vat Green 03 indanthren of industrial textile dye that is soluble in alkaline media to synthetic design dyeing cellulose fibers and proteins , as well as for printing cotton .As shown in Fig. 16.It was provided to us by the textile company Essenia in Oran «West of Algeria."The aqueous solution of Vat Green 03 indanthren was prepared from a stock solution of 1 g/L and the discharge is diluted to 0.5 mg/L , since it is very concentrated and contains other additives (caustic soda NaOH, sodium hydrosulfite $Na_2S_2O_4$) .All manipulations of the photodegradation of Vat Green 03 indanthren was conducted in a beaker of 250 mL with stirring at room temperature [20-25 °C] [17]. The materials used are prepared from and 0.5 g/L of diatomite silica doped iron nanoparticle thermally calcination at 600 °C “ DMF3X6 ” in three different pH medium (4, 7 and 10).Were introduced into the beaker , 200 mL of the dye (Vat Green 03) concentration of 20 mg/L and 0.5g of diatomite silica doped iron nanoparticle thermally calcination at 600 °C “ DMF3X6 ” adjusted the pH to 4,7, and 10 were then put the solutions in the dark under UV irradiation ultraviolet samples of 10 mL every 15 minutes to measure the pH, the sample is centrifuged (15000 rotations

/min) for one-half hour and finally measuring the absorbance on a spectrophotometer model Optizen Micrometrics . As shown in Fig.17.The Fig.17 represents the manipulation of photodegradation between (Vat Green 03 dye textile) and the used the product diatomite silica doped iron nanoparticle thermally calcination at 600 °C “ DMF3X6 ” utilize the agitator with speed 300 rotations/min in the photocatalytic reactor but the transilluminator is changed the photocatalytic reactor Transilluminator the length equal to 365 nm wave type Biometra , width of the lamp is 15 cm and a length of 30 cm , energy elimination is 45 Watt and the summarized results are shown in Fig. 18 ; Fig. 19 ; Fig. 20 and Fig.21 respectively.



Fig.17. Test of photodegradation (Vat Green 03 indanthren dye textile) in presence diatomite silica doped iron nanoparticle thermally calcination at 600 °C “ DMF3X6 ” in the photocatalytic reactor (transilluminator) The discoloration efficiency of the catalyst was calculated by the following equation Eq. (4)

$$\text{Decolourisation (\%)} = (C_0 - C) / C_0 \quad (4)$$

Here C is the concentration of Vat Green 03 indanthren solution at irradiation time of “ t ” min, and C_0 is the initial absorption at $t=0$ min.

Measurement of pH

At 60 min of reaction, It was found that increase of solution pH from 4 to 10 increased the decolorization efficiency. Fig.18 shows the effect of the pH of the medium on photodecolorization of vat green 03 Indanthren in the presence of diatomite silica doped iron nanoparticle thermally calcination at 600 °C “ DMF3X6 ” under UV irradiation of transilluminator as a function of irradiation time. The pH of vat green 03 Indanthren with diatomite silica doped iron nanoparticle thermally calcination at 600 °C “ DMF3X6 ” tends to neutral.

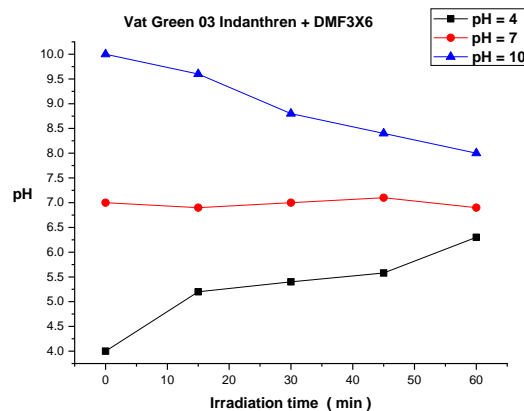


Fig.18. pH change of the mixture (Vat Green 03 indanthren + DMF3X6) over time under UV irradiation

Photodegradation kinetics

Fig.19 shows the degradation kinetics of Vat Green 03 textile dye under the UV lamp, using diatomite silica doped iron nanoparticle thermally calcination at 600 °C “ DMF3X6 ” according to the pH medium different.

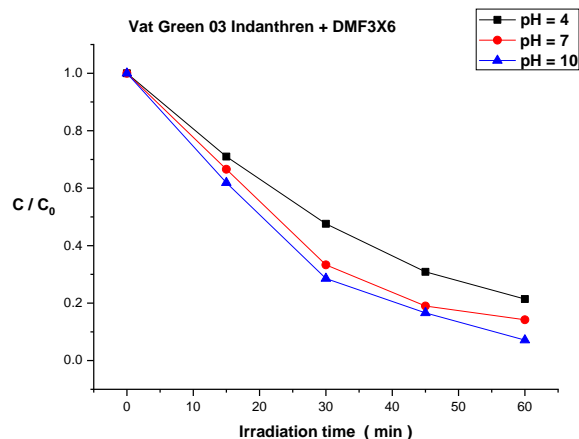


Fig.19. the degradation kinetics of Vat Green 03 textile dye using the DMF3X6

The kinetics of degradation of Vat Green 03 pennies lamp UV shows that the photoactivity using diatomite silica doped iron nanoparticle thermally calcination at 600 °C “ DMF3X6 ” is favorable for a pH equal to 4 compared to the other pH.

Reactions kinetics order

The discoloration efficiency of diatomite silica doped iron nanoparticle thermally calcination at 600 °C for vat green 03 indanthren dye was quantified by measurement of dye apparent first order rate constants under operating parameters Eq. (5) :

$$\text{Log} \frac{C_0}{C} = K_{app}t \quad (5)$$

Where K_{app} is the apparent pseudo-first order rate constant, C and C_0 are the concentrations at time “ t ” and “ $t=0$ ”, respectively .The plot of $\ln C_0/C$ against irradiation time t should give straight lines, whose slope is equal to K_{app} . In all the photodecolourisation experiments, the reaction followed first order kinetics .Plots of $\ln[C_0/C]$ versus time showed linear relationship where C is the concentration of vat green 03 indanthren remaining in the solution at irradiation time of t , and C_0 is the initial concentration at $t = 0$ min in different pH's.First order rate constants were evaluated from the slopes of $\ln[C_0/C]$ versus time plots (Fig.20).In this work, the “ k ” is calculated by linear regression shown in Fig.20. At pH= 4, the observed rate constant for the photodecolourisation of vat green 03 indanthren in the presence of diatomite silica doped iron nanoparticle thermally calcination at 600 °C “ DMF3X6 ” is $2.56 \times 10^{-2} \text{ min}^{-1}$, at pH= 7 , the observed rate constant for the photodecolourisation of vat green 03 indanthren in the presence of diatomite silica doped iron nanoparticle thermally calcination at 600 °C “ DMF3X6 ” is $3.66 \times 10^{-2} \text{ min}^{-1}$.at pH=10, the observed rate constant for the photodecolourisation of vat green 03 indanthren in the presence of diatomite silica doped iron nanoparticle thermally calcination at 600 °C “ DMF3X6 ” is 0 min^{-1} because linear regression does not pass on all the points of samples.As concluded about the observed rate constant ,the reaction followed first order kinetics at pH = 4,and at pH = 7, but at pH = 10, the reaction followed is not nor first order and nor pseudo-first order .

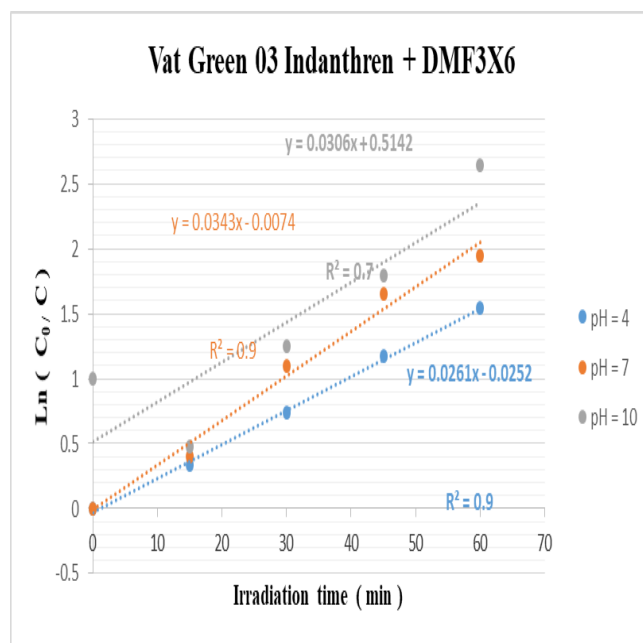


Fig.20. Effect of pH solutions on reactions kinetics order determination for photodecolourisation of vat green 03 indanthren textile dye using the diatomite silica doped iron nanoparticle thermally calcination at 600 °C “ DMF3X6 ” in function of irradiation time

Colour removal of vat green 03 indanthren

Fig.21 shows the colour removal of vat green 03 indanthren in different pH's using the diatomite silica doped iron nanoparticle thermally calcination at 600 °C “ DMF3X6 ” .At 60 min of reaction, it was verified that in pH = 4, there was a colour remove about 79 %, at pH = 7,there was a colour remove about 85 %, and at pH = 10, there was a colour remove about 92 %.It was verified that in pH = 10, there was a better colour remove about 92 %.It was observed that the vat green 03 indanthren textile dye degradation has pH dependency ,the better result is at pH = 10.

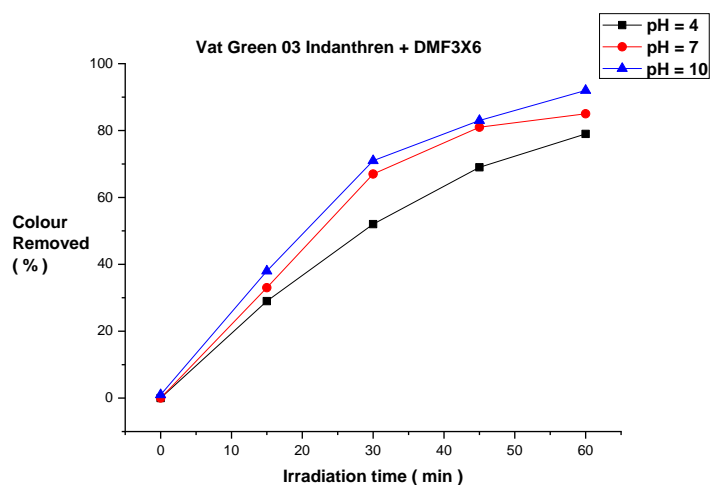


Fig.21. Colour removal of vat green 03 indanthren in different pH's using the diatomite silica doped iron nanoparticle thermally calcination at 600 °C "DMF3X6 "

IV. CONCLUSION

Synthesis of diatomite silica doped iron nanoparticle thermally calcination at 600 °C "DMF3X6 " composite has been successfully carried out based on the characterization result and applied to degrade vat green 03 indanthren dye on UV irradiation. The band gap for DMF3X6 was $E_g = 1.15$ eV by UV-visible DRS technique. It was verified that in pH = 10, there was a better colour remove about 92%. It was observed the vat green 03 indanthren textile dye degradation has pH dependency, the better result is at pH = 10.

As concluded about synthesis of diatomite silica doped iron nanoparticle thermally calcination at 600 °C "DMF3X6 " by the formation of new structure through bonding Si-O-Fe and Ti-O-Fe linkages verified by ATR-FTIR Which were responsible for its UV irradiation photocatalytic activity for photodecolourisation of vat Green 03 indanthren textile dye.

REFERENCES

- [1] F.E. Round, R.M. Crawford, D.G. Mann, *The Diatoms: Biology and Morphology of the Genera*, 1st ed., Cambridge University Press, UK, 1990.
- [2] F.L. Kadey, F. L. (1975). Diatomite. In S. J. Lefond (Ed.), *Ind. miner. rocks* (4th ed., pp. 605–635).
- [3] E. Erdem, G. Colgecen, R. Donat. The removal of textile dyes by diatomite earth, *J. Colloid Interface Sci.* 282 (2005) 314–319.
- [4] Z. Al-Qodah, W.K. Lafi, Z. Al-Anber, M. Al-Shannag, A. Harahsheh, Adsorption of methylene blue by acid and heat treated diatomaceous silica, *Desalination* 217 (2007) 212–224.
- [5] U. Schwertmann, R.M. Cornell, *Iron Oxides in the Laboratory: Preparation and Characterization*, Wiley-VCH, New York, 2000.

- [6] W. Xiong, J. Peng, Y. Hu, *Phys. Chem. Mineral.* 36 (2009) 557–566.
- [7] A. Aleboyed, H. Aleboyeh, Y. Moussa, Decolorisation of Acid Blue 74 by ultraviolet/H₂O₂, *Environ. Chem. Lett.* 1 (2003) 161–164.
- [8] M. Muruganandham, M. Swaminathan, Decolorisation of Reactive Orange 4 by Fenton and Photo-Fenton oxidation technology, *Dyes Pigments* 63 (2004) 315–321.
- [9] D.S.L. Balan, R.T.R. Monteiro, Decolorization of textile Indigo dye by ligninolytic fungi, *J. Biotechnol.* 89 (2001) 141–145.
- [10] O.K. Dalrymple, D.H. Yeh, M.A. Trotz, *J. Chem. Technol. Biotechnol.* 82 (2007) 121–134.
- [11] X.B. Ma, S.P. Wang, J.L. Gong, X. Yang, G.H. Xu, *J. Mol. Catal. A: Chem.* 222 (2004) 183–187.
- [12] A. Fernhndez, G. Lassaletta, V.M. Jimknez, A. Justo, A.R. Gonzlez-Elipe, J.-M. Herrmann, H. Tahiri, Y. Ait-Ichou, *Appl. Catal. B: Environ.* 7 (1995) 49–63.
- [13] S. Chaudhari, M. Srinivasan, 1D hollow α -Fe₂O₃ electrospun nanofibers as high performance anode material for lithium ion batteries, *J. Mater. Chem.* 22 (43) (2012) 23049.
- [14] K. Uma, N. Arjun, G.-T. Pan, T.C.K. Yang, *Appl. Surf. Sci.* 425 (2017) 377–383.
- [15] I.A. Barbosa, P.C. de Sousa Filho, D.L. da Silva, F.B. Zanardi, L.D. Zanatta, A.J.A. de Oliveira, O.A. Serra, Y. Iamamoto, *J. Colloid Interface Sci.* 469 (2016) 296–309.
- [16] C.A. Henriques, A. Fernandes, L.M. Rossi, M.F. Ribeiro, M.J.F. Calvete, M.M. Pereira, *Adv. Funct. Mater.* 26 (2016) 3359–3368.
- [17] W. Rezig, M. Hadjel, Photocatalysis degradation of vat green 03 textile dye, using the ferrihydrite-modified diatomite with TiO₂ / UV process, *Oriental journal of chemistry*, 30 (3), (2014) 993–1007; DOI: 10.13005.
- [18] Y. Al-Degs, M.A.M. Khraishah, M.F. Tutunji, Sorption of lead ions on diatomite and manganese oxides modified diatomite, *Water Res.* 35 (2001) 3724–3728.
- [19] R.O.Y. Breese, diatomite In: carr, D.D. (Ed.), *Industrial Minerals and Rocks*, SMME, Colorado, USA, pp. 397–412, 1994.
- [20] Y.G. Frolov, N.A. Shabanova, T.V. Savochkina, *Kolloidn. Zh.* 45, 509, 1983.
- [21] R. Köseoglu, F. Köksal, E. Ciftci, M. Akkurt, *J. Mol. Struct.* 733 (2005) 151–154.
- [22] W. Feng, E. Sun, A. Fujii, H. Wu, K. Niihara, K. Yoshino, Synthesis and characterization of photoconducting polyaniline-TiO₂ nanocomposite, *Bull. Chem. Soc. Jpn.* 73 (2000) 2627–2633.
- [23] D.E. Janney, J.M. Cowley, P.R. Buseck, Transmission electron microscopy of synthetic 2- and 6-line ferrihydrite. *Clay Clay Miner.* 48 (2000) 111–119.
- [24] Y. Pan, A. Brown, R. Brydson. Electron beam damage studies on 6-line ferrihydrite, *J. Phys. Conf. Ser.* (2006) 46–49.

- [25] G. Pecchi, P. Reyes, T. Lopez. R. Gomez, A. Moreno, J.L.G. Fierro. Effect of precursors on surface and catalytic properties of Fe/TiO₂ catalyst, *J. Chem Technol Biotech*, 77 (2002), 944-949.
- [26] L.G. Yan, K. Yang, R.R. Shan, T. Yan, J. Wei, S.J. Yu, H.Q. Yu, B. Du. Kinetic, isotherm and thermodynamic investigations of phosphate adsorption onto co-shell-Fe₃O₄@LDHs composites with easy magnetic separation assistance, *J. Colloid Interface Sci.* 448 (2015) 508-516.
- [27] Z.X. Jin, X.X. Wang, Y.B. Sun, Y. Ai, X.K. Wang, Adsorption of 4-n-nonylphenol and bisphenol-A on magnetic reduced graphene oxides : a combined experimental and theoretical studies, *Environ. Sci. Technol.* 49(2015)9168-9175.
- [28] Y. Hou, Z. Xu, S. Sun, Controlled synthesis and chemical conversions of FeO nanoparticles. *Angew. Chem. Int. Ed.* 46(2007) 6329-6332.
- [29] J. Majzlan, A. Navrotsky, U. Schwertmann. Thermodynamics of iron oxides: part III. Enthalpies of formation and stability of ferrihydrite (~ Fe(OH)₃), schwertmannite (~ Fe(OH)_{3/4} (SO₄)_{1/8}), and ε-Fe₂O₃, *Geochimica et Cosmochimica Acta*, 68 (5) (2004) 1049-1059.
- [30] B.A. Morrow, I.D. Gay, Adsorption on silica surfaces, *E. Papirer. Mater. Lett.* 58 (2004) 723-726.
- [31] H. Böke, S. Akkurt, S. Özdemir, E.H. Göktürk, E.N. Caner Saltik, *Mater. Lett.* 58 (2004) 723-726.
- [32] B. Bahramian, F.D. Ardejani, V. Mirkhani, K. Badii, Diatomite-supported manganese Schiff base: An efficient catalyst for oxidation of hydrocarbons, *Appl. Catalys. A: General*, 345 (2008) 97-103.
- [33] C. Chanéac, E. Tronc, J.P. Jolivet, Magnetic iron oxide-silica nanocomposites, synthesis and characterization, *J. Mater. Chem.* 6 (1996) 1905-1911.
- [34] M.I. Tejedor-Tejedor, M.A. Anderson, *Langmuir* 2 (1986) 203-210.
- [35] R. Cornell, U. Schwertmann, *Structure, Properties, Reactions, Occurrence and Uses*, VCH, Weinheim, 1996.
- [36] R.K. Iler, *The Chemistry of Silica Solubility, Polymerization, Colloid and Surface Properties and Biochemistry of Silica*, New York, 1979.
- [37] J. Wu, Y.S. Yang, J. Lin, *J. Hazard. Mater.* 127 (2005) 196-203.
- [38] C. Chanéac, E. Tronc, J.P. Jolivet, Magnetic iron oxide-silica nanocomposites, synthesis and characterization, *J. Mater. Chem.* 6 (1996) 1905-1911.
- [39] K.M. Kutláková, J. Tokarský, P. Kovár, S. Vojtěšková, A. Kovářová, B. Smetana, J. Kukutschová, P. Čapková, V. Matějka, *J. Hazard. Mater.* 188 (2011) 212-220.
- [40] B. Sahoo, S.K. Sahu, S. Nayak, D. Dhara, P. Pramanik, *Catal. Sci. Technol.* 2 (2012) 1367-1374.
- [41] X. Yang, X. Zhang, Y. Ma, Y. Huang, Y. Wang, Y. Chen. Superparamagnetic graphene oxide-Fe₃O₄ nanoparticles hybrid for controlled targeted drug carriers. *J. Mater. Chem.* 19 (2009) 2710.
- [42] S.F. Chin, K.S. Iyer, C.L. Raston. Fabrication of carbon nanotubes decorated with ultra fine superparamagnetic nano-particles under continuous flow conditions. *Lab. Chip.* 8 (2008) 439-442.
- [43] X.F. Hou, H. Ding, Y.X. Zheng, M.M. Wang, *Mater. Res. Innov.* 17(2013).
- [44] R. Zuo, G. Du, W. Zhang, L. Liu, Y. Liu, L. Mei, Z. Li, *Adv. Mater. Sci. Eng.* 2014 (2014) 7.
- [45] H. Liu, P. Li, M. Zhu, Y. Wei, Y. Sun, *J. Solid State Chem.* 180 (2007) 2121-2128.
- [46] D. Mohan, K.P. Singh, *Water Res.* 36 (2002) 2304-2310.
- [47] L. Tuhela, L. Carlson, O.H. Tuovinen, Ferrihydrite in water cells and bacterial enrichment cultures. *Water Res.* 26 (1992), 1159-1162.
- [48] R. Yezou, Contribution à l'étude des propriétés thermoplastiques des matériaux de construction cohérents et non cohérents, Thèse de Docteur-Ingénieur, INSA de Lyon, France, 1978.
- [49] D.W. Hawes, D. Feldman, D. Baru, Latent heat storage in building materials, *Energy Build.* 20 (1993) 77-86.
- [50] W. Xu, D.B. Hausner, R. Harrington, P.L. Lee, D.R. Strongin, J.B. Parise, Structural water in ferrihydrite and constraints this provides on possible structure models. *Am. Mineral.* 96 (2011), 513-520.
- [51] A. Rufus, N. Sreeju, V. Vilas, D. Philip. Biosynthesis of hematite (α-Fe₂O₃) nanostructures: size effects on applications in thermal conductivity, catalysis, and antibacterial activity. *J. Mol. Liq.* 242 (2017) 537-49.
- [52] A. Lassoued, B. Dkhil, A. Gadri, S. Ammar. Control of the shape and size of iron oxide (α-Fe₂O₃) nanoparticles synthesized through the chemical precipitation method. *Results Phys.* 7 (2017) 3007-3015.
- [53] M. Stoia, A. Tamaş, G. Rusu, J. Moroşanu. Synthesis of magnetic iron oxides from ferrous sulfate and substituted amines. *Stud Univ Babeş-Bolyai Chem.* 61 (2016).
- [54] V. Rao, A.L. Shashimohan, A.B. Biswas. Studies on the formation of γ-Fe₂O₃ (maghemite) by thermal decomposition of ferrous oxalate dihydrate. *J. Mater. Sci.* 9 (1974) 430-433.
- [55] G.W. Sears, *Anal. Chem.* 28 (1956) 1981-1983.
- [56] J. Chen, S. Yieconmi, T.G. Blaydes. Equilibrium and kinetic studies of copper adsorption by activated carbon. *Sep. Technol.* 6 (1996) 133-146.
- [57] J.P. Chen, M. Lin. Equilibrium and kinetics of metal adsorption onto a commercial H-type granular activated carbon; experimental and modelling studies. *Water Res.* 35 (2001) 2385-2394.
- [58] M.P. Dare-Edwards, A.H. Goodnough, A. Hammett, P.R. Trevellick, *J. Chem. Soc. Faraday Trans.* 9 (1983) 2027-2041.
- [59] D. Barreca, C. Massignan, S. Daolio, M. Fabrizio, C. Piccirillo, L. Armelao, E. Tondello, *Chem. Mater.* 13 (2001) 588-593.
- [60] Y.-H. Chang, C.M. Liu, H.E. Cheng, C. Chen, *ACS Appl. Mater. Interfaces* 5 (2013) 3549-3555.